Hindawi Publishing Corporation
ISRN Physical Chemistry
Volume 2013, Article ID 675138, 10 pages
http://dx.doi.org/10.1155/2013/675138

Research Article

Inefficient Vibrational Cooling of C_{60} in a Supersonic Expansion

Jacob T. Stewart,[1,2] Brian E. Brumfield,[1,3] Bradley M. Gibson,[1] and Benjamin J. McCall[4]

[1] *Department of Chemistry, University of Illinois, Urbana, IL 61801, USA*
[2] *Department of Chemistry, Emory University, Atlanta, GA 30322, USA*
[3] *Department of Electrical Engineering, Princeton University, Princeton, NJ 08544, USA*
[4] *Departments of Chemistry and Astronomy, University of Illinois, Urbana, IL 61801, USA*

Correspondence should be addressed to Benjamin J. McCall; bjmccall@illinois.edu

Received 17 September 2013; Accepted 12 November 2013

Academic Editors: M. Sliwa, D. Strout, L. Vattuone, and A. Vergara

High-resolution gas-phase infrared spectroscopy of buckminsterfullerene (C_{60}) was attempted near 8.5 μm using cavity ring-down spectroscopy. Solid C_{60} was heated in a high-temperature (~950 K) oven and cooled using an argon supersonic expansion generated from a 12.7 mm × 150 μm slit. The expected *S/N* ratio is ~140 for vibrationally cold C_{60}, but no absorption signal has been observed, presumably due to a lack of vibrational cooling of C_{60} in the expansion. Measurements of D_2O at 875 K are presented as a test of instrument alignment at high temperature and show that efficient rotational cooling of D_2O occurs in the hot oven (T_{rot} = 20 K in the expansion), though vibrational cooling does not occur. The attempted C_{60} spectroscopy is compared to previous work which showed efficient vibrational cooling of polycyclic aromatic hydrocarbons (PAHs). Possible alternative experiments for observing a cold, gas-phase spectrum of C_{60} are also considered.

1. Introduction

Ever since its discovery in 1985 [1], buckminsterfullerene (C_{60}) has been the subject of an enormous body of research (the publication of its discovery has been cited more than 8100 times at the time of writing according to Web of Science). One particular area of interest is the astrochemistry of C_{60}. C_{60} was long believed to be present in the interstellar medium (ISM) and has recently been detected via emission spectroscopy in the mid-infrared (mid-IR) [2–7]. Though C_{60} has been detected in the ISM, the mechanism by which it is formed is still under debate [8]. Obtaining an astronomical absorption spectrum of C_{60} would yield additional information about the abundance and temperature of C_{60} in the ISM, which could provide useful information in determining the formation mechanism. Unfortunately, astronomical searches for absorption from cold gas-phase C_{60} are hampered by the lack of a high-resolution gas-phase laboratory spectrum of any of the four infrared active vibrational bands of C_{60}.

A rotationally resolved spectrum of C_{60} would also be of great fundamental interest. The acquisition of such a spectrum would be a significant milestone in the field of molecular spectroscopy, as C_{60} would be the largest and most symmetric molecule to be observed with rotational resolution. In addition, due to boson exchange symmetry restrictions on the overall symmetry of the molecular wave function there are many rotational levels in the ground and vibrationally excited state that are rigorously forbidden to exist [9, 10]. Such missing levels will manifest as "gaps" in the normal progression of rovibrational lines.

Despite great interest in a high-resolution spectrum of C_{60}, a rotationally resolved, gas-phase absorption spectrum of C_{60} has not yet been observed. There are several obstacles which must be overcome to record such a spectrum. First, it is difficult to generate a gas-phase sample of C_{60}. C_{60} has negligible vapor pressure at room temperature and must be heated to temperatures in excess of 875 K to reach a vapor pressure on the order of 10–100 mTorr [15]. Second, C_{60} has 174 vibrational modes, which leads to a large vibrational partition function at even modest temperatures (see Figure 1). Cooling the vibrational degrees of freedom will be critical for observing a fundamental vibrational band. Finally, it is necessary to have a sensitive, high-resolution spectrometer in the mid-IR to observe the relatively small amount of gas-phase sample.

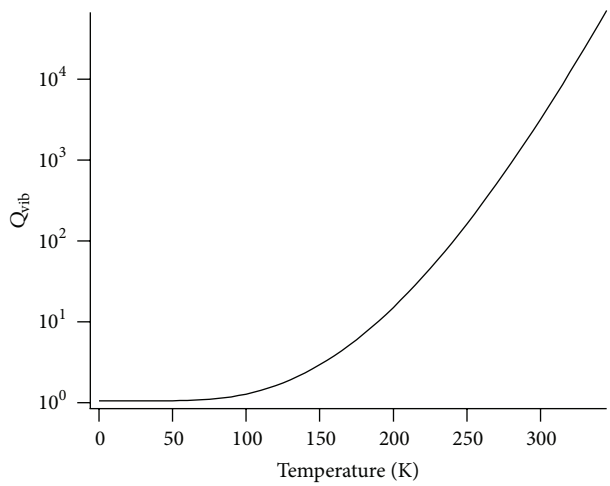

Figure 1: Plot of C_{60} vibrational partition function (on a logarithmic scale) versus temperature. The vibrational frequencies used in the calculation were obtained from [16].

We have developed an experiment which attempts to address these obstacles. We have built a high-temperature oven source which has been used to generate C_{60} vapor. To attempt to relax the vibrational degrees of freedom, the hot C_{60} vapor has been cooled using a supersonic expansion. The supersonic jet is then probed using continuous wave cavity ring-down spectroscopy (cw-CRDS) [18]. We have attempted to observe the 8.5 μm band due to the availability of quantum cascade laser (QCL) sources at this wavelength and also because this band coincides with an atmospheric window, permitting ground-based astronomical observations. The cavity ring-down spectrometer has already been tested by carrying out high-resolution spectroscopy of methylene bromide [19] and pyrene [13]. Despite multiple spectral searches under a variety of expansion source conditions, no absorption signals from C_{60} have yet been detected.

Previous work has shown effective vibrational cooling of large molecules, such as polycyclic aromatic hydrocarbons (PAHs), in supersonic expansions [13, 14, 20]. In contrast to this previous work, our lack of signal indicates that the vibrational degrees of freedom are not effectively cooled in C_{60}. We will discuss the details of our experiment and also briefly discuss measurements of D_2O made in the heated oven, which show good rotational cooling, but no vibrational cooling. We will also compare our current experiment to the previous work showing good vibrational cooling of other large molecules. Finally, we will present possible alternative experiments which may allow observation of a high-resolution absorption spectrum of C_{60}.

2. Materials and Methods

2.1. QCL-Based Cavity Ring-Down Spectrometer. Our high-resolution mid-IR spectrometer has been described in detail previously [18, 19], so here we present only a brief overview of the instrument. Mid-IR light near 8.5 μm is generated using a QCL supplied by collaborators in the Gmachl group at Princeton. The frequency of the emitted light can be tuned from ~1180 to 1200 cm^{-1} by changing the temperature of the laser and the current applied to the QCL. Light from the QCL is sent through an optical isolator to an optical cavity where we perform cw-CRDS to record the infrared absorption spectrum of our sample. To calibrate our spectra we utilize an absorption cell filled with SO_2 to provide absolute frequency calibration and a mid-IR wavemeter for relative frequency calibration.

2.2. Vaporization Source and Expansion Seeding. We have constructed a high-temperature oven which we used to produce gas-phase C_{60}. The oven is described in detail in our previous work on pyrene [13]. The oven is made from stainless steel with attached strip heaters to provide heating and is capable of operating under vacuum at temperatures up to 975 K for many hours. To produce gas-phase C_{60} for spectroscopy, solid C_{60} (MER Corporation, 99 + % purity) was loaded into the oven, which was then placed in a vacuum chamber and surrounded by an aluminum heat shield. The oven was heated by applying current to the strip heaters using variable transformers, which gave us coarse control over the temperature of the oven. The oven temperature was monitored using a thermocouple inserted into the interior of the oven. Once we had achieved the desired temperature (~ 950 K) a stream of Ar gas was passed through the oven and generated a continuous supersonic expansion of the Ar/C_{60} mixture through a 12.7 mm × 150 μm slit; the expansion was then probed with our spectrometer. Effective vaporization of C_{60} in the oven was verified by measuring the mass of C_{60} in the oven following a set of scans, and also by deposition of C_{60} on the walls of our vacuum chamber. The alignment between the supersonic expansion from the vaporization source and the optical cavity was verified in separate experiments through spectroscopy of D_2O. In these experiments, trace D_2O (Cambridge Isotope Laboratories, 99.9% D) was seeded into the Ar flow and was passed through the vaporization source as it was being operated at temperatures similar to those used when vaporizing solid C_{60}.

2.3. Signal-to-Noise Estimation for C_{60}. Knowledge of where to scan in frequency space to detect the first signal from the 8.5 μm vibrational band of C_{60} is critical. Restricting the search window allowed us to focus on varying experimental parameters instead of trying to cover a large spectral region. The only gas-phase measurements come from observations of infrared emission at ~1000 K [21, 22]. The estimated band center position was 1169.1 cm^{-1} [21], but this estimate is likely red-shifted due to the contribution from hot bands, whose emission frequencies are shifted due to vibrational anharmonicity. Low-temperature (15 K) measurements of C_{60} films assign the center position to 1183.7 cm^{-1} [23], while Ar matrix spectroscopy yields 1184.8 cm^{-1} [24]. Measurements in para-H_2 (p-H_2), considered the least perturbing matrix host, place the center position of the vibrational band at 1184.7 cm^{-1} [10]. Because the frequency shift between Ar and p-H_2 matrix hosts for a spectral feature is generally comparable to the frequency shift between gas-phase and p-H_2, we feel confident

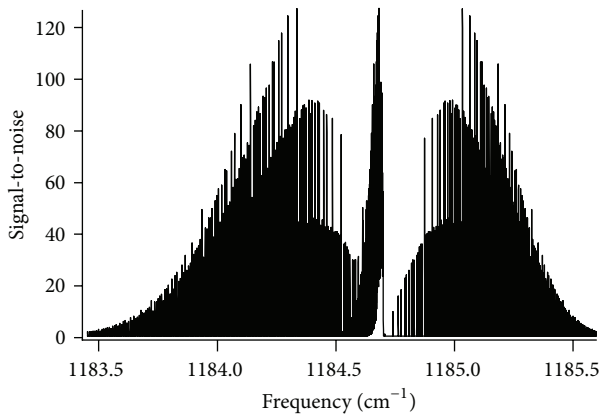

Figure 2: Plot of calculated S/N versus frequency. The S/N was calculated at T_{rot} = 20 K, T_{vib} = 0 K, B'' = 0.0028 cm^{-1}, B' = 0.002795 cm^{-1}, ζ = −0.0319, oven temperature of 955 K, and a mass loss of 2.0 g/hr, corresponding to a probed number density of $^{12}C_{60}$ in the expansion of 1.7×10^{12} cm^{-3}. The assumed noise level was 1.0 ppm and the linewidth for the transitions was set to 0.0004 cm^{-1}. The largest value of S/N for a single rovibrational transition is ~130. These parameters are similar to our experimental parameters for attempt 1 listed in Table 1. The value for ζ comes from [17].

that the peak of the 8.5 μm absorption band should be near the p-H_2 matrix value of 1184.7 cm^{-1}.

We have simulated the 8.5 μm C_{60} vibrational band at high resolution, following the approach of Sogoshi et al. [10]. As noted by Sogoshi et al., the appearance of the spectrum will be dependent on the change of the rotational constant from the ground to the excited vibrational state as well as the Coriolis coupling constant ζ. If the change in rotational constant is small, there will be a prominent Q-branch. If the change is large (on the order of 1%), there could be a prominent R-branch head. Because we do not know if either of these cases will happen in the actual experimental spectrum, we base our signal-to-noise (S/N) estimates on observing a single rovibrational transition. To estimate our expected signal, we use a theoretical value for the band strength of the 8.5 μm band [25] of 25 km/mol. Our estimates assume a vibrational temperature of 0 K. We will discuss the importance of vibrational excitation in Section 3.3.

Estimating the expected S/N for C_{60} absorption using our experimental apparatus parallels calculations that we carried out to estimate vibrational cooling of pyrene in a previous publication [13]. We begin with the following formula for estimating the S/N for a single rovibrational transition:

$$\frac{S}{N} = \frac{n_z f S' L_{jet}}{\Delta\tilde{\nu}\,(\sigma_{NEA})}. \quad (1)$$

In this equation, n_z is the number density of $^{12}C_{60}$ in units of cm^{-3} at a distance z from the slit, f is the ratio of the line intensity for a single transition (factoring in Boltzmann statistics) divided by the sum of all the line intensities, S' is the calculated band strength in cm/molecule, L_{jet} is the length of the expansion in cm, $\Delta\tilde{\nu}$ is the linewidth of the transition in cm^{-1}, and σ_{NEA} represents the noise equivalent fractional absorption of the spectrometer. By evaluating each of these parameters for our instrument and this band of C_{60}, we can calculate an expected S/N for our experiment.

To estimate the number density, we use the rate of mass loss from the oven per unit time, combined with the velocity of molecules in the expansion. We account for the fact that not all of the molecules in the expansion will overlap with the TEM_{00} mode of the cavity and be probed by our spectrometer and that only 51.5% of the sample is $^{12}C_{60}$. In our previous work with pyrene, we have measured that only ~20% of the molecules in the expansion overlap with the TEM_{00} mode of the ring-down cavity [13]. Because there is little expansion along the axis of the slit, we assume that L_{jet} equals the length of the slit (12.7 mm) and can find the number density of molecules probed by our spectrometer:

$$n_{probed} = \frac{0.20 \times 0.515 \times \dot{N}_{C_{60}}}{2\omega_0 \times L_{slit} \times v_{max}}, \quad (2)$$

where $\dot{N}_{C_{60}}$ is the rate of molecules lost from the oven per second, ω_0 is the beam waist of the TEM_{00} mode, L_{slit} is the length of the slit, and v_{max} is the flow velocity of molecules in the expansion (for further details on the derivation of this expression, we refer readers to the supporting information for [13]). We estimate $\dot{N}_{C_{60}}$ by measuring the amount of C_{60} before and after heating the sample and recording the length of time for which the expansion was on. ω_0 can be calculated from the radius of curvature of our ring-down mirrors, the length of the cavity, and the wavelength of light in the cavity [26]. For our setup, ω_0 is equal to 1.1 mm. v_{max} for the expansion can be found from the temperature and mass of carrier gas atoms in the expansion [27].

We can now use (1) to calculate our expected S/N for the slit expansion, using a 0.0004 cm^{-1} (12 MHz) linewidth, which we have observed in slit expansions of methylene bromide and pyrene [13, 19]. Figure 2 displays the estimated S/N for the entire vibrational band for the measured mass loss at 955 K (2 g/hr) with the slit 6 mm from the cavity axis. The largest estimated S/N for a single rovibrational transition is ~130 (for the $P(60)$, $Q(60)$, and $R(60)$ lines).

3. Results and Discussion

3.1. Search for the C_{60} Spectrum. Our attempts to observe C_{60} are summarized in Table 1. We also attempted 6 spectroscopic searches for C_{60} using a smaller oven with both a slit and pinhole expansion, which are discussed in detail in [28], but the work presented here represents our best attempts with a high calculated S/N and complete frequency coverage of where the band is expected to be. We decided to use a slit expansion because of the narrower linewidth of transitions and the greater vibrational cooling due to the larger number of collisions that occur in a slit expansion. Our attempts were performed at three different backing pressures and all three attempts covered the entire frequency region between 1184 and 1186 cm^{-1} where we expect to observe the C_{60} vibrational band. In all attempts a $S/N > 70$ was anticipated; however, we saw no evidence of absorption due to C_{60} in any of these

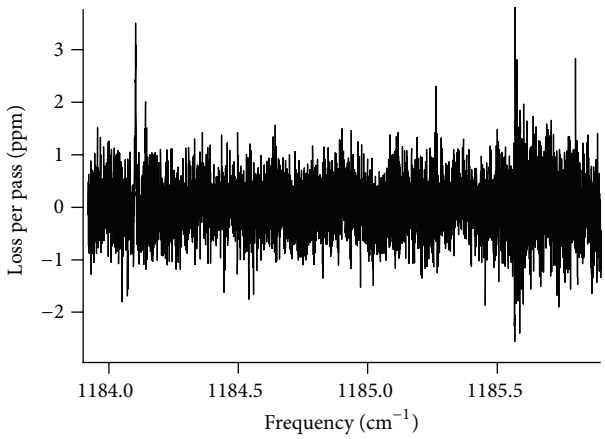

Figure 3: Representative absorption spectrum of the Ar/C_{60} expansion from 1184 to 1186 cm^{-1}. This plot is from attempt 3 listed in Table 1. Baseline drifts have been corrected by use of polynomial fitting and subtraction. Periodic fringing was removed by Fourier transforming the spectrum, eliminating the most intense frequency components, and then inverse Fourier transforming the result to retrieve the spectrum. Similar data processing was used for all attempts where periodic fringing was observed. The spikes near 1185.6 cm^{-1} are due to noise and were not reproducible. The line at 1184.1 cm^{-1} is due to absorption by water vapor in the vacuum chamber. The standard deviation of the spectrum is 0.6 ppm.

Table 1: Summary of attempted absorption spectroscopy of C_{60}. The measured mass loss rate for each attempt was used to calculate S/N. The mass loss rates were 2.0 g/hr for attempts 1 and 2 and 0.7 g/hr for attempt 3. For all attempts, the supersonic expansion was probed 6 mm downstream from the exit of the slit.

Attempt	T_0 (K)	P_0 (torr)	NEA (ppm)[a]	Estimated S/N[b]
1	955	150	1.0	130
2	955	500	0.9	140
3	965	1900	0.6	74

[a]NEA: noise equivalent absorption.
[b]These values represent the largest S/N value for a single rovibrational transition at T_{rot} = 20 K and T_{vib} = 0 K following the analysis presented in Section 2.3.

searches. An example of our spectra is presented in Figure 3, which comes from attempt 3 in Table 1.

As can be seen in Table 1, the mass loss rate for our attempts decreased from attempts 1 and 2 to attempt 3, even though all three attempts were performed at approximately the same oven temperature. The same sample was used for attempt 3 after it had been used for attempts 1 and 2, and the reduced mass loss rate for attempt 3 is indicative of sample decomposition. We also observed that after attempt 3, our sample was no longer soluble in toluene and had become conductive, even though pure C_{60} is an insulator. Further characterization by CHN analysis revealed that the recovered sample was ~89% carbon by weight, with the elemental composition of the remaining mass as yet unknown. This implies that the actual mass of C_{60} lost over the course of attempts 1, 2, and 3 was higher than reported, but without elemental analysis between attempts we cannot say when this C_{60} mass loss occurred. Because of the decomposition of our sample, the reported S/N ratios in Table 1 represent average values for the expected S/N over the course of a scan, as the mass loss rate was decreasing as we were scanning our spectrometer.

The observed reduction in the mass loss of C_{60} from the source is consistent with prior reports in the literature. In a previous study on the thermal decomposition of C_{60}, Sundar et al. observed that C_{60} held at 975 K for an extended period of time (24 h) decomposed to amorphous carbon [29]. Other publications have also observed a similar reduction in vapor pressure over time when measuring the vapor pressure of C_{60} at elevated temperatures [15, 30, 31]. This effect has been attributed to residual solvent impurities of benzene, toluene, or hexane resulting from the HPLC separation of the raw fullerene sample produced by the carbon arc method [32]. Heating the impure sample above 750 K then results in a chemical transformation of C_{60} to a different substance, such as amorphous carbon, with a reduced vapor pressure.

3.2. High Temperature Measurements of D_2O. Because of the high temperatures involved in producing gas-phase C_{60}, we were concerned that the alignment of our optical cavity with our oven might be affected by thermal expansion or other heating effects. To eliminate this possibility, we observed absorption spectra of D_2O in expansions from our oven at similar temperatures as our C_{60} searches. There are many lines of the bending mode as well as a hot band within the spectral coverage of our spectrometer, which also allowed us to monitor the rotational and vibrational temperature of D_2O molecules in the high temperature supersonic expansion.

We introduced a small amount of D_2O into an Ar slit expansion and observed low-lying states which were populated in the expansion. We observed the $1_{11} \leftarrow 0_{00}$ transition of the (010) ← (000) band of D_2O at 1199.79 cm^{-1} with the oven at 875 K to determine if alignment effects could be responsible for failure to observe C_{60}. We were easily able to observe the line in the expansion, and displacing the oven vertically only caused a slight change in the intensity of the line, consistent with the molecular distribution we measured with pyrene. This indicates that the extreme temperatures of our oven are not affecting the alignment of our ring-down cavity and preventing the observation of a C_{60} absorption signal.

Measuring several transitions of D_2O in the expansion from the hot oven permitted calculation of both the rotational and vibrational temperatures for D_2O. Table 2 presents a list of the transitions that we measured in the (010) ← (000) and (020) ← (010) vibrational bands of D_2O. Each line was measured 5 times and the average intensity for each line was used for all temperature calculations. Figure 4 shows a Boltzmann plot for both the fundamental and hot band transitions, showing that the rotational temperature of the D_2O molecules is ~20 K in both the ground and excited vibrational states. From this we see that even though the expansion originated in an oven at 875 K, the rotational degrees of freedom are cooled efficiently. On the other hand, the strength of the hot band lines is consistent with a vibrational temperature >1000 K. The hot vibrational temperature for D_2O is not surprising,

Table 2: List of observed D_2O transitions. Rotational levels are denoted in the usual way (J_{K_a,K_c}). The listed frequencies are from [11, 12].

Vibrational band	Transition	Frequency (cm^{-1})
(010) ← (000)	$1_{11} \leftarrow 0_{00}$	1199.793
	$2_{02} \leftarrow 1_{11}$	1194.038
	$2_{11} \leftarrow 2_{02}$	1193.255
	$3_{12} \leftarrow 3_{03}$	1198.536
(020) ← (010)	$1_{11} \leftarrow 0_{00}$	1181.311
	$3_{13} \leftarrow 2_{02}$	1199.154
	$2_{20} \leftarrow 2_{11}$	1192.497
	$2_{21} \leftarrow 2_{12}$	1199.690
	$4_{04} \leftarrow 3_{13}$	1198.379

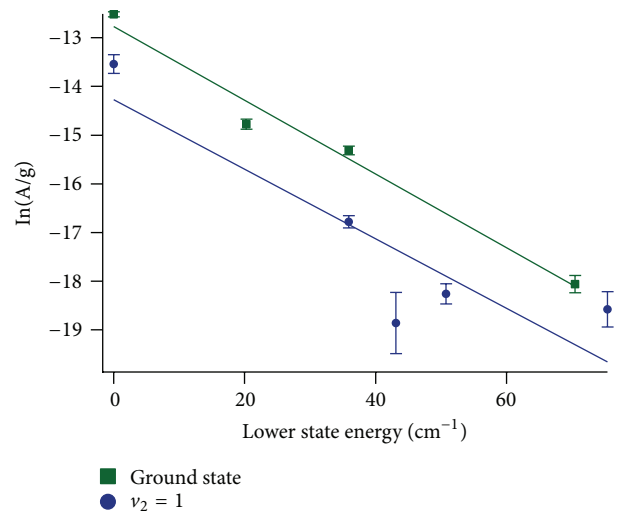

Figure 4: Boltzmann plot of D_2O rotational levels observed in the supersonic jet at 875 K. The error bars indicate 3σ deviations from the average for each data point. The calculated rotational temperatures from the linear fits are 19 ± 2 K for the ground vibrational state (green squares) and 20 ± 6 K for the $\nu_2 = 1$ vibrational state (blue circles). The uncertainties in the temperatures are 1σ values.

considering that the lowest energy vibration in the molecule lies at ~1178 cm^{-1}. Even at an oven temperature of 875 K, this is almost twice the value of k_BT (608 cm^{-1} at 875 K), and vibrational modes with energies significantly higher than k_BT do not effectively relax to the ground vibrational state in a supersonic expansion [33].

3.3. Vibrational Partition Function and Importance of Vibrational Cooling. From the material presented in Section 2.3 describing the method of calculating the experimental S/N, we can see that if the C_{60} molecules are cooled vibrationally in the supersonic expansion, we would anticipate observing an absorption signal even if there is not a strong R-branch head or Q-branch. Therefore, the most likely explanation for our lack of observed signal is that we are not achieving sufficient vibrational cooling of C_{60}. For us to observe absorption from the C_{60} molecules, they must be in the ground vibrational state. The fraction of molecules in the ground vibrational state (assuming a Boltzmann distribution) is given by the expression

$$f_0 = \frac{e^{-E_0/(k_B T_{\text{vib}})}}{Q_{\text{vib}}}, \tag{3}$$

where E_0 is the energy of the ground vibrational state, T_{vib} is the vibrational temperature, and Q_{vib} is the vibrational partition function. If we express the vibrational energies relative to $E_0 = 0$, (3) simply becomes the inverse of the partition function. Because C_{60} has 174 vibrational degrees of freedom, its vibrational partition function increases rapidly with increasing temperature (see Figure 1), meaning that very few molecules occupy the ground vibrational state at high temperatures. Even at a vibrational temperature as low as 190 K, only 1 in 10 C_{60} molecules will be in the ground vibrational state, leading to an order of magnitude decrease for an absorption signal. If we assume that the lack of vibrational cooling is the primary cause preventing us from observing C_{60}, we can calculate a lower limit for T_{vib} in the expansion using our expected S/N and (3). Our expected signal is proportional to f_0, so if our expected S/N is 140 (as in attempt 2 in Table 1), f_0 must be decreased by at least a factor of 140 for us not to observe the signal. This means that Q_{vib} must be at least 140, which would correspond to $T_{\text{vib}} \simeq 250$ K. It should be noted that this lower limit of 250 K assumes a Boltzmann distribution for the vibrational levels, which is likely not the case in a supersonic expansion.

Previous studies have shown that large molecules (specifically PAHs) can be effectively cooled in supersonic expansions [14]. Our own recent measurements of pyrene using the experimental setup described in this paper indicated that pyrene was cooled to $T_{\text{vib}} = 23$–111 K [13]. It is useful to compare these previous studies with our current attempted spectroscopy to ascertain why we were unable to observe C_{60} absorption in our expansion.

Vibrational cooling of large molecules seeded in a supersonic expansion of a monatomic carrier gas proceeds by transferring vibrational energy from the large molecule to translational energy in the expansion by collisions with the carrier gas (V-T transfer). Because of this, the number of collisions that a molecule experiences in the supersonic expansion will have a significant effect on the amount of vibrational cooling that is possible in the expansion. We have estimated the number of two-body hard sphere collisions which occur in our attempted C_{60} spectroscopy and previous work on PAHs by our group [13] and Amirav et al. [14]. The estimated number of collisions for our work and the work of Amirav et al. [14] is found in Table 3. The details of our calculations are outlined in the following paragraphs.

The first step in estimating the number of collisions in a supersonic expansion is to describe the temperature, density, and velocity of molecules in the expansion. These properties

Table 3: Estimated number of two body hard sphere collisions experienced by large molecules seeded in an argon supersonic expansion. The first three entries in the table are from the attempted C_{60} spectroscopy reported in this work. The pyrene entry is from our previous work observing pyrene in the same experimental setup which we used to attempt C_{60} spectroscopy [13]. The remaining entries are from laser induced fluorescence spectroscopy of the listed PAHs performed by Amirav et al. [14]. The listed pressures for the PAHs were sufficient to produce vibrationally cold molecules ($T_{vib} \lesssim 100$ K). The C_{60} and pyrene expansions used a 12.7 mm × 150 μm slit. For the work of Amirav et al. [14] all expansions used a 150 μm diameter pinhole. Further details on how the number of collisions was calculated can be found in the article text.

Molecule	T_0 (K)	P_0 (torr)	Nozzle type	Number of collisions
C_{60} (att. 1)	955	150	Slit	320
C_{60} (att. 2)	955	500	Slit	1100
C_{60} (att. 3)	965	1900	Slit	4000
Pyrene	430	150	Slit	560
Anthracene	410	270	Pinhole	600
Tetracene	485	175	Pinhole	360
Pentacene	550	250	Pinhole	500
Ovalene	630	300	Pinhole	620

Table 4: Hard sphere radii used to compute the mean free path of molecules in the supersonic expansion.

Species	Radius (Å)
Ar	1.88
C_{60}	5.0
Pyrene	4.0
Anthracene	3.8
Tetracene	4.2
Pentacene	4.6
Ovalene	5.1

are given by the following equations for the centerline of the expansion, which are reproduced from [34]

$$T(z) = T_0\left(1 + \frac{\gamma - 1}{2}M^2\right)^{-1},$$
$$n(z) = n_0\left(1 + \frac{\gamma - 1}{2}M^2\right)^{-1/(\gamma-1)}, \quad (4)$$
$$v(z) = M\sqrt{\frac{\gamma k_B T_0}{m}}\left(1 + \frac{\gamma - 1}{2}M^2\right)^{-1/2}.$$

In these equations, z represents the distance from the nozzle along the centerline of the expansion, T_0 and n_0 are the temperature and number density of the gas prior to the expansion, γ is the heat capacity ratio (which is 5/3 for the argon expansions we consider here), M is the Mach number of the expansion, and m is the mass of the gas. Because the large molecule is only a minor constituent of the gas being expanded, we assume that the properties of the expansion can be approximated as that of a pure argon expansion. To use these equations, we also need to know the value of M as a function of z; equations to do so for both slit and pinhole expansion sources are provided in [34].

The next step in calculating the number of collisions is to calculate the mean free path of the large molecules in the expansion. To do so, we use a hard sphere model, which gives the usual equation:

$$\lambda(z) = \frac{1}{\sqrt{2}\pi\left(r_{large} + r_{Ar}\right)^2 n(z)}, \quad (5)$$

where $\lambda(z)$ is the mean free path as a function of distance from the expansion nozzle and r_{large} and r_{Ar} are the hard sphere radii for the large molecule and argon atoms, respectively. Because C_{60} is roughly a sphere, we can simply use the van der Waals radius of C_{60} for r_{large} in this equation, but the PAHs studied by us and Amirav et al. are far from spherical. To get a rough approximation of a hard sphere radius for these species, we used values for the minimum and maximum projected cross-sections of the molecules as given in the chemicalize.org database from ChemAxon [35]. To obtain a hard sphere radius, we averaged the minimum and maximum projected cross-sections for the PAHs and then calculated an effective radius based on the average cross section of the molecule. While this is certainly not exact, it should give a rough estimate of the relative size of the PAHs for computing the mean free path and seems to give reasonable results. The hard sphere radii which we used to compute the mean free path are listed in Table 4.

We can then calculate the average frequency of two-body collisions of the large molecule with Ar atoms in the expansion by dividing the average speed of the molecules by the mean free path. We assume that the translational temperature of the large molecules is thermalized with the translational temperature of the Ar atoms and calculate the average speed according to

$$s(z) = \sqrt{\frac{8k_B T(z)}{\pi\mu}}, \quad (6)$$

where μ is the reduced mass of the Ar and large molecule. Using the above equations, we can calculate the collision frequency at any point z along the centerline of the expansion. We calculated the collision frequency in steps of 1.5 μm from $z = 0$ to 6 mm along the expansion for all of the molecules and conditions listed in Table 3. We then calculated the number of collisions at each point by calculating the velocity of the expansion to determine how long the molecules were within each 1.5 μm section and then multiplying that time by the collision frequency. We then added together the number of collisions calculated for each of these 1.5 μm sections from $z = 0$ to 6 mm to give the total number collisions listed in Table 3. We use a maximum of 6 mm because that is where the expansion was probed in our work and in the work of Amirav et al. [14].

From Table 3, we can see that the PAHs were vibrationally cooled after undergoing an average of 360–620 collisions with Ar. In our attempted C_{60} spectroscopy, the C_{60} molecules underwent an average of 320, 1100, and 4000 collisions with

Table 5: Vibrational partition function, average vibrational energy (above zero-point energy) in cm^{-1}, frequency of the lowest energy vibrational mode, and energy to collision ratio for the molecules listed in Table 2 at the temperatures listed in that table. The calculated values for our D_2O measurements from Section 3.2 are also included for comparison.

Molecule	Q_{vib}	E_{vib} (cm^{-1})	ν_{min} (cm^{-1})	E_{vib} /collisions
C_{60} (att. 1)	1.3×10^{28}	56000	267	174
C_{60} (att. 2)	1.3×10^{28}	56000	267	50
C_{60} (att. 3)	3.0×10^{28}	57000	267	14
Pyrene	4.0×10^{3}	4000	99	7
Anthracene	1.5×10^{3}	3200	91	5
Tetracene	1.0×10^{6}	6400	56	18
Pentacene	2.5×10^{9}	10000	38	21
Ovalene	8.6×10^{13}	18000	61	29
D_2O	1.20	260	1178	0.8

Ar for attempts 1, 2, and 3 in Table 1, respectively. For attempts 1 and 2, the number of collisions is similar to the number of collisions for the PAH molecules, while the much higher backing pressure for attempt 3 increased the number of collisions by an order of magnitude compared to attempt 1. While the C_{60} molecules underwent a similar number of collisions as the PAHs, or significantly more for attempt 3, we have seen that this was insufficient to produce vibrationally cold C_{60}, which would have been observable with our spectrometer. To try to understand why this might be the case, we can compare the vibrational properties of these molecules.

Theoretical harmonic vibrational frequencies for all of the PAHs listed in Table 3 can be found in the PAH IR Spectral Database [36], which come from the original data of Langhoff [37]. We have used these vibrational frequencies to calculate the vibrational partition functions of the PAHs and C_{60} at high temperature before being cooled by supersonic expansion. Using the vibrational partition function, we can also calculate the amount of vibrational energy in an average molecule at high temperature. These values are presented in Table 5 for all of the molecules we have been considering. The first thing to notice is the incredibly large partition functions for these molecules at elevated temperatures, especially for C_{60} and ovalene. According to (3), this means that on average only 1 in 10^{28} molecules of C_{60} is in the ground vibrational state before the expansion. Table 5 also shows that these molecules have a large amount of vibrational energy (over 50000 cm^{-1} for C_{60}) that must be transferred into the supersonic expansion to cool them vibrationally. For the PAHs, we have seen that it is possible to transfer this energy in the hundreds of collisions that occur in the expansion. We can divide the vibrational energies in Table 5 by the collision numbers in Table 3 to calculate an energy to collision ratio to get an idea of how much energy would need to be removed in an average collision to cool the molecule. This ratio is listed in the last column of Table 5. For the vibrationally cold PAH molecules, an average collision carried away 5–30 cm^{-1} of energy. For our attempted C_{60} spectroscopy, the energy to collision ratio is significantly higher than this for attempt 1, slightly higher for attempt 2, and right in the range of the PAHs for attempt 3.

Looking at these values, it is somewhat surprising that C_{60} was not efficiently cooled using a supersonic expansion for attempts 2 and 3. Considering the previous work with PAHs, it appears that there should be enough collisions to carry away the vibrational energy for these attempts. One possible reason why C_{60} was not efficiently cooled is that the lowest energy vibrational mode for C_{60} is at 267 cm^{-1}, which is significantly higher than the lowest modes for the PAHs (see Table 5). To completely cool the molecule to the ground vibrational state, energy must be transferred from the lowest vibrational mode into translational energy. The efficiency of V-T transfer decreases as the energy gap increases, making it more difficult for modes with higher energy to be completely cooled. As an extreme example of this, we can consider the D_2O spectroscopy presented in Section 3.2. We have calculated the vibrational properties for D_2O following the same procedure as for C_{60} and the PAHs, using vibrational frequencies from [38]. The results are listed in Table 5 and show that the amount of vibrational energy for a small molecule at high temperature is much lower than the large molecules we have been considering. At a temperature of 875 K and a backing pressure of ~300 torr, the average number of hard sphere collisions for a D_2O molecule in the expansion is 310 (using a hard sphere radius of 1.6 Å), which gives an energy to collision ratio of 0.8. Even though this ratio is significantly lower than for all of the PAHs, we observed substantial population in the (010) state, indicating no cooling of this vibrational mode. This lack of cooling is a direct consequence of the fact that the lowest energy mode lies so high in energy.

Another possibility is that the extremely large size of C_{60} is causing a significant velocity slip effect to occur because of the large difference in mass between the C_{60} molecules and the Ar carrier gas [14]. While this does not seem to be a problem for the previous work on ovalene, C_{60} is about 2 times heavier than ovalene. This problem would be easily remedied by using a heavier carrier gas such as Kr or Xe, which would more closely match the mass of C_{60}. We did not try a heavier gas because of the increased cost of these gases compared to Ar, especially when used continuously, as in our experiment. For future attempts to observe C_{60}, it may be worth the extra expense to try the heavier rare gases to reduce the velocity slip effect.

Finally, it is worth noting that other molecules have been observed to have anomalously low cooling efficiency in supersonic expansions. In particular, Sulkes observed that benzene

displays a lack of collision-induced vibrational relaxation in He and Ar expansions, despite the fact that substituted benzene derivatives showed excellent cooling under similar conditions [39]. Sulkes attributed this to a lack of efficient cooling via orbiting resonances; it is conceivable that a similar effect is occurring with C_{60}.

3.4. Alternative Methods for Producing Gas-Phase C_{60}. It would be preferable to produce C_{60} vapor at a much lower temperature than is possible in our oven. Doing so would significantly decrease the vibrational partition function and vibrational energy of the molecules prior to the supersonic expansion. For example, if C_{60} vapor could be produced at a temperature similar to our pyrene work (430 K), then the vibrational partition function would be only 5×10^7 and an average molecule would only have 11000 cm^{-1} of vibrational energy, which would be quite similar to the PAHs that were observed by Amirav et al. This should make it much easier to cool the C_{60} molecules to the ground vibrational state.

We are aware of three possible methods for producing C_{60} vapor at lower temperatures: supercritical fluid expansion, laser desorption, and collisional cooling in the gas-phase. In the supercritical fluid expansion method the C_{60} sample would be dissolved in a supercritical fluid. It has been demonstrated that C_{60} can be dissolved in supercritical toluene, or to a lesser extent in supercritical carbon dioxide containing toluene as a co-solvent [40, 41]. Assuming a 1 : 1 volume ratio of CO_2 to toluene, the critical temperature is ~450 K. Decreasing the toluene content will lower the critical temperature, though this would be at the expense of solubility. It will be necessary to optimize the toluene content for our particular needs. We would likely employ an argon sheath-flow continuous expansion source, as in [42].

A laser desorption/supersonic expansion source has been successfully employed for resonant two-photon ionization measurements of C_{60} [43, 44], but the vibrational temperature of the vapor produced was not directly observed. Likewise, while it has been shown that laser desorption can volatilize large molecules with pre-expansion vibrational temperatures below what one would expect for thermal vaporization [45, 46], the temperatures achievable are molecule- and surface-dependent and as yet unknown for C_{60}. As such, the viability of a laser desorption source is difficult to assess without further experiments.

The final method to discuss for producing cold gas-phase C_{60} relies upon the modified use of a gas-phase aggregation cluster source [47] to collisionally cool isolated C_{60} molecules. In an aggregation source the hot vapor from the heated sample is entrained in a flow of noble gas that is cooled by collisions with the walls inside the source that are kept at 77 K using liquid nitrogen cooling [48, 49]. A collimated molecular beam of cold sample clusters is produced by passing the flow out of the source through a nozzle. While normally such sources are used to efficiently produce large clusters of molecules or atoms, it has been shown that cold isolated C_{60} molecules can be produced by keeping the gas-phase number density of C_{60} low through reduction of the temperature of the sample oven [47]. By operating the aggregation source in this way it was possible to collect two-photon resonant ionization spectra of C_{60} with an estimated vibrational temperature <80 K [47].

Although we expect all of the proposed methods to be superior to our current oven in terms of vibrational temperature, we also expect them to produce significantly lower number densities of gas-phase C_{60}. Based on reports of supercritical fluid extractions of C_{60} [40, 41], we anticipate that the number density produced by a supercritical fluid expansion would be two orders of magnitude lower than that of our current oven. Studies where laser desorption [43, 44] or collisional cooling [47] was used do not report gas-phase C_{60} number densities; however, the C_{60} number densities generated using these methods will be considerably lower than the number density produced using a supercritical fluid. Assuming that C_{60} can be efficiently cooled in a supercritical fluid expansion, we will need to implement high repetition rate CRDS [50] to account for the low C_{60} number density. Depending on the repetition rate achieved, doing so would improve S/N by a factor of 10–20. If C_{60} does not cool completely or the number density is lower than anticipated, noise-immune cavity-enhanced optical heterodyne molecular spectroscopy (NICE-OHMS) detection could be implemented instead, improving our signal-to-noise ratio by as much as three orders of magnitude [51]. This route would also significantly increase the technical complexity of our spectrometer.

4. Conclusions

Obtaining a high-resolution gas-phase spectrum of C_{60} represents a significant challenge for molecular spectroscopy. We have attempted to obtain such a spectrum using a highly sensitive cw-CRDS spectrometer but were unable to detect any absorption signal from C_{60}. We have shown that an absorption signal should be expected with our current experimental setup if we are able to vibrationally cool C_{60}. Our lack of signal is most likely due to the fact that we must heat our sample to >950 K to obtain sufficient vapor pressure for spectroscopy, which leads to an incredibly large vibrational partition function because of the large size of C_{60}. We have compared these results with previous work that has shown efficient vibrational cooling of large polycyclic aromatic hydrocarbons. To overcome this problem it will be necessary to produce gas-phase C_{60} at much lower temperatures so that the vibrational degrees of freedom can be cooled. While there may exist alternative methods that are capable of generating a cold gas-phase sample, these methods will result in low number densities of C_{60}. The low C_{60} number density will require the use of more sensitive and complex absorption spectroscopy techniques than cw-CRDS to enable collection of a rotationally resolved spectrum.

Conflict of Interests

The authors have no direct financial relations with the commercial identities named in this work.

Acknowledgments

The authors would like to thank the Gmachl group at Princeton for providing the quantum cascade lasers which have made this work possible. The authors also thank Gregory S. Girolami for useful discussions about decomposition of the C_{60} sample. Their efforts to observe the spectrum of C_{60} have been supported by the NASA Laboratory Astrophysics Program (APRA NNG05GE59G), a Camille and Henry Dreyfus New Faculty award, a Packard Foundation Fellowship, and the University of Illinois. Jacob T. Stewart has been supported by a Robert C. and Carolyn J. Springborn Fellowship from the University of Illinois.

References

[1] H. W. Kroto, J. R. Heath, S. C. O'Brien, R. F. Curl, and R. E. Smalley, "C_{60}: buckminsterfullerene," *Nature*, vol. 318, no. 6042, pp. 162–163, 1985.

[2] J. Cami, J. Bernard-Salas, E. Peeters, and S. E. Malek, "Detection of C_{60} and C_{70} in a young planetary nebula," *Science*, vol. 329, no. 5996, pp. 1180–1182, 2010.

[3] K. Sellgren, M. W. Werner, J. G. Ingalls, J. D. T. Smith, T. M. Carleton, and C. Joblin, "C_{60} in reflection nebulae," *The Astrophysical Journal Letters*, vol. 722, no. 1, pp. L54–L57, 2010.

[4] D. A. García-Hernández, A. Manchado, P. García-Lario et al., "Formation of fullerenes in H-containing planetary nebulae," *The Astrophysical Journal Letters*, vol. 724, no. 1, pp. L39–L43, 2010.

[5] D. A. García-Hernández, N. K. Rao, and D. L. Lambert, "Are C_{60} molecules detectable in circumstellar shells of R Coronae Borealis stars?" *The Astrophysical Journal*, vol. 729, no. 2, p. 126, 2011.

[6] D. A. García-Hernndez, S. Iglesias-Groth, J. A. Acosta-Pulido et al., "The formation of fullerenes: clues from new C_{60}, C_{70}, and (Possible) planar C_{24} detections in Magellanic cloud planetary nebulae," *The Astrophysical Journal Letters*, vol. 737, no. 2, article L30, 2011.

[7] O. Berné and A. G. G. M. Tielens, "Formation of buckminsterfullerene (C_{60}) in interstellar space," *Proceedings of the National Academy of Sciences of the United States of America*, vol. 109, no. 2, pp. 401–406, 2012.

[8] J. Bernard-Salas, J. Cami, E. Peeters, A. P. Jones, E. R. Micelotta, and M. A. T. Groenewegen, "On the excitation and formation of circumstellar fullerenes," *The Astrophysical Journal*, vol. 757, no. 1, p. 41, 2012.

[9] R. Saito, G. Dresselhaus, and M. S. Dresselhaus, "Hindered rotation of solid $^{12}C_{60}$ and $^{13}C_{60}$," *Physical Review B*, vol. 50, no. 8, pp. 5680–5688, 1994.

[10] N. Sogoshi, Y. Kato, T. Wakabayashi et al., "High-resolution infrared absorption spectroscopy of C_{60} molecules and clusters in parahydrogen solids," *Journal of Physical Chemistry A*, vol. 104, no. 16, pp. 3733–3742, 2000.

[11] C. Camy-Peyret, J.-M. Flaud, A. Mahmoudi, G. Guelachvili, and J. W. C. Johns, "Line positions and intensities in the ν_2 band of D_2O improvied pumped D_2O laser frequencies," *International Journal of Infrared and Millimeter Waves*, vol. 6, no. 3, pp. 199–233, 1985.

[12] R. A. Toth, "HDO and D_2O low pressure, long path spectra in the 600–3100 cm^{-1} region II. D_2O line positions and strengths," *Journal of Molecular Spectroscopy*, vol. 195, no. 1, pp. 98–122, 1999.

[13] B. E. Brumfield, J. T. Stewart, and B. J. McCall, "Extending the limits of rotationally resolved absorption spectroscopy: pyrene," *Journal of Physical Chemistry Letters*, vol. 3, pp. 1985–1988, 2012.

[14] A. Amirav, U. Even, and J. Jortner, "Cooling of large and heavy molecules in seeded supersonic beams," *Chemical Physics*, vol. 51, pp. 31–42, 1980.

[15] V. Piacente, G. Gigli, P. Scardala, A. Giustini, and D. Ferro, "Vapor pressure of C_{60} buckminsterfullerene," *The Journal of Physical Chemistry*, vol. 99, no. 38, pp. 14052–14057, 1995.

[16] J. Menendez and J. B. Page, *Light Scattering in Solids VIII: Fullerenes, Semiconductor Surfaces, Coherent Phonons*, Springer, Berlin, Germany, 2000.

[17] D. E. Weeks and W. G. Harter, "Rotation-vibration scalar coupling χ coefficients and spectroscopic band shapes of buckminsterfullerene," *Chemical Physics Letters*, vol. 176, no. 2, pp. 209–216, 1991.

[18] B. E. Brumfield, J. T. Stewart, S. L. Widicus Weaver et al., "A quantum cascade laser cw cavity ringdown spectrometer coupled to a supersonic expansion source," *Review of Scientific Instruments*, vol. 81, no. 6, Article ID 063102, 2010.

[19] B. E. Brumfield, J. T. Stewart, and B. J. McCall, "High-resolution spectroscopy of the ν_8 band of methylene bromide using a quantum cascade laser," *Journal of Molecular Spectroscopy*, vol. 266, no. 1, pp. 57–62, 2011.

[20] A. Amirav, U. Even, and J. Jortner, "Absorption spectroscopy of ultracold large molecules in planar supersonic expansions," *Chemical Physics Letters*, vol. 83, no. 1, pp. 1–4, 1981.

[21] C. I. Frum, R. Engleman Jr., H. G. Hedderich, P. F. Bernath, L. D. Lamb, and D. R. Huffman, "The infrared emission spectrum of gas-phase C_{60} (buckmisterfullerene)," *Chemical Physics Letters*, vol. 176, no. 6, pp. 504–508, 1991.

[22] L. Nemes, R. S. Ram, P. F. Bernath et al., "Gas-phase infrared emission spectra of C_{60} and C_{70}. Temperature-dependent studies," *Chemical Physics Letters*, vol. 218, no. 4, pp. 295–303, 1994.

[23] B. Chase, N. Herron, and E. Holler, "Vibrational spectroscopy of C_{60} and C_{70} temperature-dependent studies," *The Journal of Physical Chemistry*, vol. 96, no. 11, pp. 4262–4266, 1992.

[24] R. E. Haufler, J. Conceicao, L. P. F. Chibante et al., "Efficient production of C_{60} (buckminsterfullerene), $C_{60}H_{36}$, and the solvated buckide ion," *The Journal of Physical Chemistry*, vol. 94, no. 24, pp. 8634–8636, 1990.

[25] D. A. Dixon, B. E. Chase, G. Fitzgerald, and N. Matsuzawa, "Prediction of the fundamental vibrational frequencies for C_{60} by local density functional theory," *The Journal of Physical Chemistry*, vol. 99, no. 13, pp. 4486–4489, 1995.

[26] K. Busch and M. Busch, Eds., *Cavity-Ringdown Spectroscopy: An Ultratrace Absorption Measurement Technique*, American Chemical Society, Washington, DC, USA, 1999.

[27] O. F. Hagena, "Nucleation and growth of clusters in expanding nozzle flows," *Surface Science*, vol. 106, no. 1–3, pp. 101–116, 1981.

[28] B. E. Brumfield, *Development of a quantum cascade laser based spectrometer for high-resolution spectroscopy of gas phase C_{60} [Ph.D. thesis]*, University of Illinois at Urbana-Champaign, 2011.

[29] C. S. Sundar, A. Bharathi, Y. Hariharan, J. Janaki, V. Sankara Sastry, and T. S. Radhakrishnan, "Thermal decomposition of C_{60}," *Solid State Communications*, vol. 84, no. 8, pp. 823–826, 1992.

[30] A. Popović, G. Dražič, and J. Marsel, "Mass spectrometric investigations of fullerenes. I. vapour pressure over the C_{60}/C_{70} binary system," *Rapid Communications in Mass Spectrometry*, vol. 8, no. 12, pp. 985–990, 1994.

[31] E. Schönherr, K. Matsumoto, and M. Freiberg, "On the evaporation of C_{60} in vacuum and inert gases at temperatures between 830 K and 1050 K," *Fullerene Science and Technology*, vol. 7, no. 3, pp. 455–466, 1999.

[32] P. F. Coheur, M. Carleer, and R. Colin, "The absorption cross sections of C_{60} and C_{70} in the visible-UV region," *Journal of Physics B*, vol. 29, no. 21, pp. 4987–4995, 1996.

[33] M. E. Sanz, M. C. McCarthy, and P. Thaddeus, "Vibrational excitation and relaxation of five polyatomic molecules in an electrical discharge," *Journal of Chemical Physics*, vol. 122, no. 19, Article ID 194319, 2005.

[34] D. R. Miller, *Atomic and Molecular Beam Methods*, vol. 1, Oxford University Press, New York, NY, USA, 1988.

[35] "Chemicalize.org was used for geometry prediction of pyrene, anthracene, tetracene, pentacene, ovalene, and D_2O," April 2013, http://www.chemaxon.com/.

[36] C. W. Bauschlicher Jr., C. Boersma, A. Ricca et al., "The NASA Ames polycyclic aromatic hydrocarbon infrared spectroscopic database: the computed spectra," *The Astrophysical Journal Supplement Series*, vol. 189, no. 2, pp. 341–351, 2010.

[37] S. R. Langhoff, "Theoretical infrared spectra for polycyclic aromatic hydrocarbon neutrals, cations, and anions," *The Journal of Physical Chemistry*, vol. 100, no. 8, pp. 2819–2841, 1996.

[38] T. Shimanouchi, *Tables of Molecular Vibrational Frequencies Consolidated*, vol. 1 of *National Bureau of Standards*, Washington, DC, USA, 1972.

[39] M. Sulkes, "Anomalously small jet-cooling of benzene: absence of efficient low-energy collision-induced vibrational relaxation," *Chemical Physics Letters*, vol. 119, no. 5, pp. 426–430, 1985.

[40] K. Jinno and C. Kohrikawa, "Supercritical and subcritical fluid extraction of fullerenes from carbon soot," *Chimica Oggi*, vol. 16, no. 1-2, pp. 9–15, 1998.

[41] S. Saim, K. C. Kuo, and D. L. Stalling, "Supercritical fluid extraction of fullerenes C_{60} and C_{70} from carbon soot," *Separation Science and Technology*, vol. 28, no. 8, pp. 1509–1525, 1993.

[42] C. H. Sin, M. R. Linford, and S. R. Goates, "Supercritical fluid/supersonic jet spectroscopy with a sheath-flow nozzle," *Analytical Chemistry*, vol. 64, no. 2, pp. 233–238, 1992.

[43] R. E. Haufler, Y. Chai, L. P. F. Chibante et al., "Cold molecular beam electronic spectrum of C_{60} and C_{70}," *The Journal of Chemical Physics*, vol. 95, no. 3, pp. 2197–2199, 1991.

[44] R. E. Haufler, L.-S. Wang, L. P. F. Chibante et al., "Fullerene triplet state production and decay: R2PI probes of C_{60} and C_{70} in a supersonic beam," *Chemical Physics Letters*, vol. 179, no. 5-6, pp. 449–454, 1991.

[45] P. Voumard and R. Zenobi, "Laser-induced thermal desorption of aniline from silica surfaces," *The Journal of Chemical Physics*, vol. 103, no. 15, pp. 6795–6805, 1995.

[46] J.-Y. Zhang, D. S. Nagra, and L. Li, "Molecular cooling and supersonic jet formation in laser desorption," *Analytical Chemistry*, vol. 65, no. 20, pp. 2812–2818, 1993.

[47] K. Hansen, R. Müller, P. Brockhaus, E. E. B. Campbell, and I. V. Hertel, "Resonant two-photon ionisation spectroscopy of C_{60}," *Zeitschrift fur Physik D*, vol. 42, no. 3, pp. 153–155, 1997.

[48] U. Zimmermann, N. Malinowski, U. Näher, S. Frank, and T. P. Martin, "Producing and detecting very large clusters," *Zeitschrift für Physik D*, vol. 31, no. 1, pp. 85–93, 1994.

[49] C. Ellert, M. Schmidt, C. Schmitt, T. Reiners, and H. Haberland, "Temperature dependence of the optical response of small, open shell sodium clusters," *Physical Review Letters*, vol. 75, no. 9, pp. 1731–1734, 1995.

[50] R. Z. Martínez, M. Metsälä, O. Vaittinen, T. Lantta, and L. Halonen, "Laser-locked, high-repetition-rate cavity ringdown spectrometer," *Journal of the Optical Society of America B*, vol. 23, no. 4, pp. 727–740, 2006.

[51] M. S. Taubman, T. L. Myers, B. D. Cannon, and R. M. Williams, "Stabilization, injection and control of quantum cascade lasers, and their application to chemical sensing in the infrared," *Spectrochimica Acta A*, vol. 60, no. 14, pp. 3457–3468, 2004.